

Quality Comparison of Free-of-Charge Global DSMs: ALOS AW3D30, TanDEM-X 12 m, TanDEM-X EDEM, TanDEM-X 90 m, and Sentinel-1

Umut Gunes Sefercik ¹, Karsten Jacobsen ²

¹Dept. of Geomatics Engineering, Gebze Technical University, Kocaeli, Türkiye - sefercik@gtu.edu.tr

²Institute of Photogrammetry and Geoinformation, Leibniz University Hannover, Hannover, Germany - jacobsen@ipi.uni-hannover.de

Keywords: DSM, Quality, ALOS AW3D30, TanDEM-X 12 m, TanDEM-X EDEM, TanDEM-X 90 m, SENTINEL-1.

Abstract

Digital Surface Model (DSM), with the height of the visible surface, is the most detailed digital 3D cartographic representation of Earth visible surface including all natural and man-made objects with X, Y planimetric coordinates and altitude Z. DSMs are frequently used in many areas such as agriculture, forestry, architecture, archaeology, disaster monitoring, especially in mapping, and this situation brings with it a high demand. In order to meet these demands, many DSM generation techniques have been developed based on the use of remote sensing technologies. Satellite technologies are used in the generation of DSMs of large areas such as provinces, countries, and continents due to the limited availability of airborne technologies. In this context, the global DSM concept, which has the potential to cover the whole world, has emerged with the beginning of the 2000s. Global DSMs have advantages and disadvantages against each other depending on the sensing principle and properties of the images used for their generation. This study aims to compare the qualities of the mostly preferred free global DSMs worldwide, produced with different sensing principles and image properties, with reference model-based visual and statistical analyses. In the analyses, the qualities of the commercial (free for scientific use) TanDEM-X 12 m (TDM12) and the free ALOS World 3D 30 m (AW3D30), TanDEM-X 30 m edited DEM (TDM EDEM) and TanDEM-X 90 m (TDM90) global DSMs were evaluated using a photogrammetric reference DSM with 5 m grid. Sentinel-1 DSM was also generated with 30 m point spacing and included in the investigations due to availability of free scenes worldwide which can be used for the generation of DSMs globally. The results demonstrated that the quality of the evaluated DSMs was TDM12 > TDM EDEM > AW3D30 > Sentinel-1 > TDM90. Generated height error maps which illustrate the pixel-based height differences between evaluated and reference DSMs revealed all the incoherent areas.

1. Introduction

Following the successful completion of the shuttle radar topography mission (SRTM) between February 11 to 22, 2000, the acquisition of digital surface model (DSM) covering the entire world except the polar regions (from 56° South to 60° North of the equator) brought the concept of "Global DSM" to the scientific literature and a large number of global DSM productions have been carried out with various satellite missions to date (Sefercik and Jacobsen, 2006). Global DSMs provide satisfactory data that enables applications covering large areas to be easily implemented. Until 2010, SRTM, ASTER and SPOT global DSMs were quite popular, however, with the integration of TanDEM-X satellite to TerraSAR-X by German Space Agency (DLR) in 2010, bistatic global DSM products of TanDEM-X mission became the focus of attention in scientific studies (Jacobsen 2012; Jacobsen and Passini, 2010; Yastikli et al., 2014; Wessel et al., 2018; Sefercik et al., 2020). In addition, ALOS World 3D with 30 m spacing (AW3D30) based on ALOS stereo pairs was generated by Japan Aerospace Exploration Agency (JAXA). Moreover, DSMs have also been generated with Sentinel-1 worldwide achievable synthetic aperture radar (SAR) images (Nikolakopoulos and Kyriou, 2015; Stamatiou et al., 2018; Sefercik et al., 2018). TanDEM-X and AW3D30 global DSM data are free-of-charge for scientific use as well as the Sentinel-1 SAR images of the European Space Agency (ESA).

The data used for the production of global DSMs are produced by space-borne remote sensing technologies, such as optical imaging and interferometric SAR (InSAR), which have completely different sensing principles and image characteristics. While optical imaging dependent on sunlight and requires cloud free condition, SAR uses signal transmitting and receiving

antennas that generate their own illumination energy and can provide data both during the day and at night with cloud penetration capability. On the other hand, object description in optical images is much stronger than in SAR images by means of multispectral data acquisition ability. In addition, the image acquisition geometries of these two imaging principles are completely different. For worldwide coverage stereo or tri-stereo satellites, as ALOS, are required or in case of InSAR usually single-pass interferometric SAR for 3D data acquisition like SRTM and TanDEM-X, while Sentinel-1 (Hounam and Werner, 1999; Sefercik and Yastikli, 2016) uses multi-pass interferometry with some disadvantages. The topography has a significant effect on the quality of a DSM. Terrain slope influences the accuracy and especially Radar in mountainous area is affected by layover, and foreshortening (Chen et al., 2018).

In this study, we analyse TanDEM-X 12 m (TDM12), AW3D30, TanDEM-X Edited DEM (TDM EDEM) and TanDEM-X 90 m (TDM90) global DSMs, and a DSM based on Sentinel-1 by comparison with a reference DSM with 5 m point spacing.

2. Study Area and Materials

The study area Tut district locates at the west part of Adiyaman Province, Türkiye. Open, built-up, forest, and water land classes are dominant in the area. The topography is a bowl-type, and very steep in the Northern and Southern parts where the elevation reaches up to 1150 m. The topographic structure and settlement areas are stable and do not show any significant change over time. Figure 1 shows the study area and the frequency distribution of elevation. The number of trees and building are limited in the test area, so that the DSM is close to a digital terrain model (DTM).

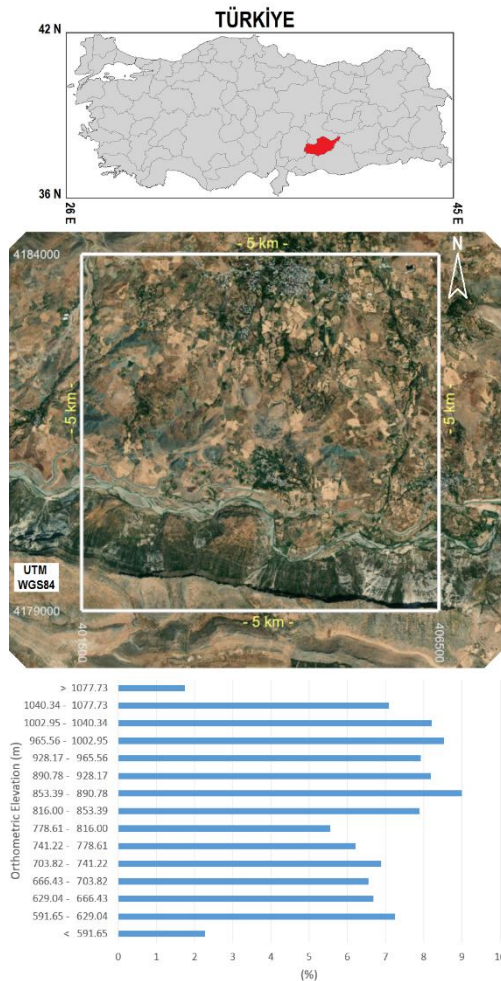


Figure 1. Study area and distribution of orthometric elevation.

2.1 Reference and Global DSMs

The reference DSM was provided from Republic of Turkey, Ministry of National Defence, Directorate General for Mapping. It has 5 m original point spacing and was generated by aerial photogrammetry with 30 cm GSD aerial photos taken in 2013.

German TDM12, TDM EDEM, TDM90 global DSMs were generated with multiple bistatic single-pass InSAR technique using the advantage of simultaneous image acquisition of TerraSAR-X and TanDEM-X twin satellites which are operated in a helix orbital geometry. In this geometry, the distance between both satellites is shortest in the poles and farthest in the equator (120 m to 500 m). With the advantage of known geometry, the baseline parameters of the InSAR image-pairs are constantly estimated. Furthermore, with the advantage of single-pass InSAR, bistatic image-pairs are not affected by atmospheric decorrelation. Therefore, a significant quality increase has been achieved in TanDEM-X mission compared to DSMs obtained with multi-pass InSAR technique from TerraSAR-X. Figure 2 shows the bistatic single-pass InSAR image acquisition and helix geometry of TanDEM-X mission. In this study, the commercial TDM12 global DSM was provided from Republic of Türkiye, Ministry of National Defence, Directorate General for Mapping like the photogrammetric reference DSM. TDM EDEM and TDM90 global DSMs were achieved from DLR EOC Geoservice. The TDM12 global DSM was generated with stripmap mode SAR images (3-6 m spatial resolution) collected between 2013 and 2016 with horizontal transmit and receive

polarization (Krieger et al., 2007, Wessel, 2016). 30 m TDM EDEM is an edited version of TDM12 global DSM to have a full and clean coverage of all Earth's landmasses from pole to pole. TDM90 is also a free version of TDM12 global DSM with reduced spacing of 3 arcseconds (~ 90 m at the equator).

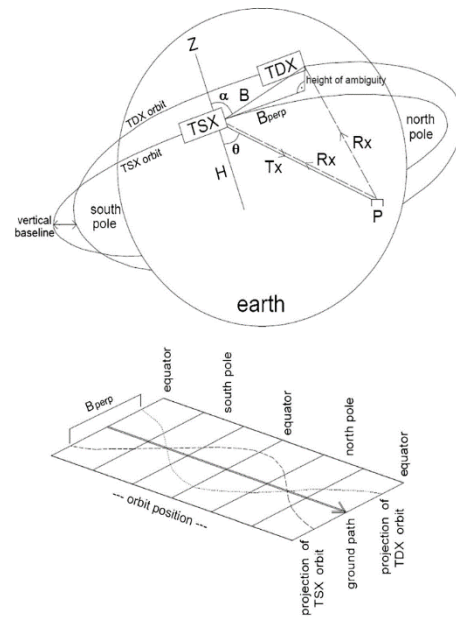


Figure 2. Bistatic single-pass InSAR image acquisition and helix orbital geometry of TanDEM-X mission.

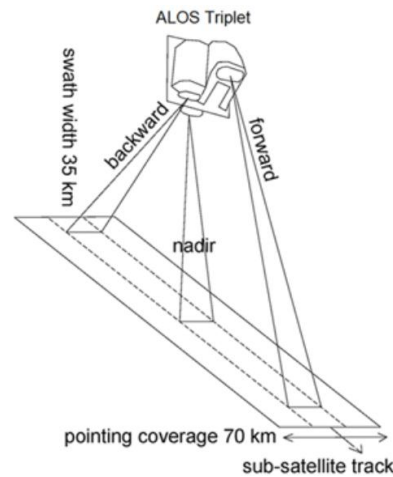


Figure 3. Triplet imaging geometry of ALOS satellite.

The AW3D30 global DSM was provided from JAXA EORC service. JAXA generated AW3D30 based on 3 million images collected by PRISM-camera system on the ALOS satellite operated from 2006 to 2011. PRISM images have 2.5 m ground sampling distance (GSD) and 35 km swath. The combination of the forward and backward cameras of PRISM has a height to base relation of 1.0, corresponding to a very large angle of convergence, optimal for open and flat areas. Figure 3 illustrates the geometry of ALOS satellite when achieving triplet images.

Sentinel-1 SAR satellite was launched in 2014 by ESA and could be used for a global DSM by multi-pass InSAR imaging. To make a trustworthy interpretation when comparing with global DSMs, an image-pair from 2016 was achieved from Copernicus Data Space Ecosystem and used for DSM generation. In the selection of the image-pair, baselines between candidate images

were calculated first. Because, optimum perpendicular baseline should be between 150-300 m to generate a qualified Sentinel-1 DSM (Hidayatulloh et al., 2022). The <150 m perpendicular baseline decreases signal-to-noise ratio (SNR) which is sensitive to atmospheric artifacts. In the interferometric processing, VV polarization images were preferred due to having more energy and lower noise (i.e. high SNR). Table 1 shows the properties of used Sentinel-1 SAR images. The perpendicular baseline between the image-pair was 166 m.

Properties	Image 1 (master)	Image 2 (Slave)
Mission	Sentinel-1A	
Product Type	SLC	
Acquisition Mode	IW	
Time	11/05/2016 17:47:07.399	13/12/2016 17:42:32.644
Relative Orbit	116	
Pass	Ascending	
Antenna Pointing	Right	
Polarization	VH, VV	
Resolution (m)	Azimuth: 13.93 Range: 2.93	
Baseline (m)	166	

Table 1. Properties of Sentinel-1 image-pair used for DSM generation.

3. Methodology

3.1 Preparation of Global DSMs

The reference DSM and TDM12, AW3D30, TDM EDEM, and TDM90 global DSMs were achieved as GeoTIFF files in geographic coordinates. First, they were converted to Universal Transverse Mercator (UTM) Zone 37 North coordinate system and World Geodetic System 1984 (WGS84) datum, subset into the region of interest and saved as ASCII files utilizing ENVI software. Also the free GDAL-translate could be used for the same processes.

For the generation of Sentinel-1 DSM, required interferometric processing steps were applied in ESA SNAP tool developed for Sentinel data processing. In theory, the minimum original point spacing of a DSM derived from remotely sensed data should be $\sim 3 \times \text{GSD}$; otherwise, the amount of data will be insufficient for rasterization and the quality of the generated model decreases due to loss of vertical accuracy by interpolation (Baltsavias 1999; Jacobsen 2012; Sefercik et al. 2015). In accordance with this significant criteria, considering 13 m azimuth resolution of the master and slave SAR images, 30 m point spacing was applied for the generated DSM. Figure 4 shows the interferometric processing workflow used in Sentinel-1 DSM generation.

The elevation datum of all global DSMs was checked and it was determined that generated Sentinel-1 and TDM90 DSMs have ellipsoidal elevations while TDM12, AW3D30 and TDM EDEM are orthometric. Accordingly, geoid undulation was calculated as 28.8 m by utilizing Turkish Geoid 2003 (TG03) in the study area and Sentinel-1 and TDM90 were converted to orthometric heights. Finally, regular gridded global DSMs were generated in Surfer software after preparations, as it would be possible also with the free GDAL-translate.

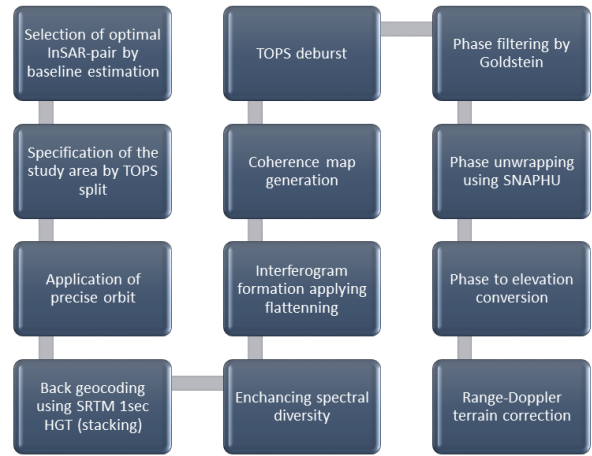


Figure 4. Interferometric processing workflow used in DSM generation.

3.2 Quality Assessment and Comparison of Global DSMs

The qualities of free-of-charge global DSMs was assessed utilizing reference model-based visual and statistical comparison approaches implemented in BLUH and LISA software. In statistical approaches, first the horizontal offsets between evaluated global DSMs and the reference DSM were determined by area-based cross correlation and eliminated by horizontal shifting. Horizontal offsets can be occurred due to different sensing geometries, image characteristics, DSM generation and interpolation techniques or national datum effects. For a correct vertical quality assessment, the compared DSMs have to fit exactly horizontally.

After achieving 100% horizontal fit, the absolute vertical accuracies of the global DSMs were calculated using the standard deviation (SZ) and normalized median absolute deviation (NMAD) of the height differences from the reference DSM (equation 1-3).

$$SZ = \sqrt{\frac{\sum_{i=1}^n (\Delta Z_i - \mu)^2}{n - 1}} \quad (1)$$

$$MAD = \tilde{X}_i [|\Delta Z_i - \tilde{X}_j(Z_j)|] \quad (2)$$

$$NMAD = 1.4826 \times (MAD) \quad (3)$$

Where n is the compared number of points in the DSMs; ΔZ is the height differences and μ is the arithmetic mean of the ΔZ (bias). \tilde{X}_j is the median of ΔZ univariate data set ($\Delta Z_1, \Delta Z_2, \Delta Z_3, \dots, \Delta Z_n$) and \tilde{X}_i is the median of absolute values of the ΔZ data set from \tilde{X}_j . NMAD is the normalization of MAD to 68% probability of normal distribution by factor 1.4826. To improve the confidence level in the absolute vertical accuracy results, the global DSM points which have >50 m height difference from the corresponding reference DSM were excluded in the analyses.

In the study, another statistical approach is the relative vertical accuracy (RSZ) assessment which shows the correlation between neighbouring points of the global DSMs. The used RSZ formulation is available in equation 4 where D describes the distance groups, D_l and D_u is the lower and upper range of the

group and n_p is the number of point combinations in the distance group. DZ_i and DZ_j are closely neighboured point heights. In the RSZ analyses, 1st to 10th pixel neighbourhood of each point was applied (point spacing \times 10).

$$RSZ = \sqrt{\frac{\sum(DZ_i - DZ_j)^2}{2 \times n_p}} \quad , \quad \begin{matrix} D_l < D \\ < D_u \end{matrix} \quad (4)$$

For visual interpretation of height differences (discrepancies) between global DSMs and the reference DSM, color-coded height error map (HEM) were produced with equation (5). With the advantage of HEMs, the influence of different land classes on the accuracy were revealed.

$$HEM = DSM_{GLOBAL} - DSM_{REFERENCE} \quad (5)$$

The quality of a DSM can be assessed considering two main parameters as the accuracy and the morphologic description potential. Accordingly, another visual approach is the generation of contour lines which demonstrates the morphologic representation capability of the DSMs. Considering the elevation distribution in the study area, contour lines were generated with 20 m height interval and 100 m contour lines were marked as bold. The structure of the contour lines is another indicator to interpret relative accuracy of the evaluated models.

4. Results

Figure 5 shows the reference DSM and evaluated TDM12, AW3D30, TDM EDEM, Sentinel-1 and TDM90 DSMs with height (h) scales. In the reference DSM, thanks to 5 m point spacing, all land classes, including open, built-up, forest areas and water (Göksu stream), are described in detail. With 12 m point spacing, TDM12 also represents significant details. The visual representation performance of Sentinel-1 DSM is not as high as AW3D30 and TDM EDEM although having same grid spacing (30 m). This is because Sentinel-1 images have an azimuth resolution of approximately 14 m, while AW3D30 is obtained from the 2.5 m ALOS imaging and TanDEM-X from the 3-6 m stripmap imaging mode.

Table 2 shows the eliminated offsets between evaluated DSMs and the reference DSM. The first issue that stands out here is that the horizontal offsets of all models in both X and Y directions are under one pixel. Except Sentinel-1, all global DSMs have isotropic offsets. In Sentinel-1, the directions of the offsets are inverse and lesser in comparison with other DSMs. The offsets in AW3D30 and the TDM EDEM are very similar.

Shifted DSM	Offset in X (m)	Offset in Y (m)
TDM12 (12 m)	-8.166	7.769
AW3D30 (30 m)	-11.080	10.814
TDM EDEM (30 m)	-13.747	14.157
Sentinel-1 (30 m)	0.182	-2.069
TDM90 (90 m)	-43.216	36.997

Table 2. Eliminated planimetric offsets between evaluated DSMs and reference DSM.

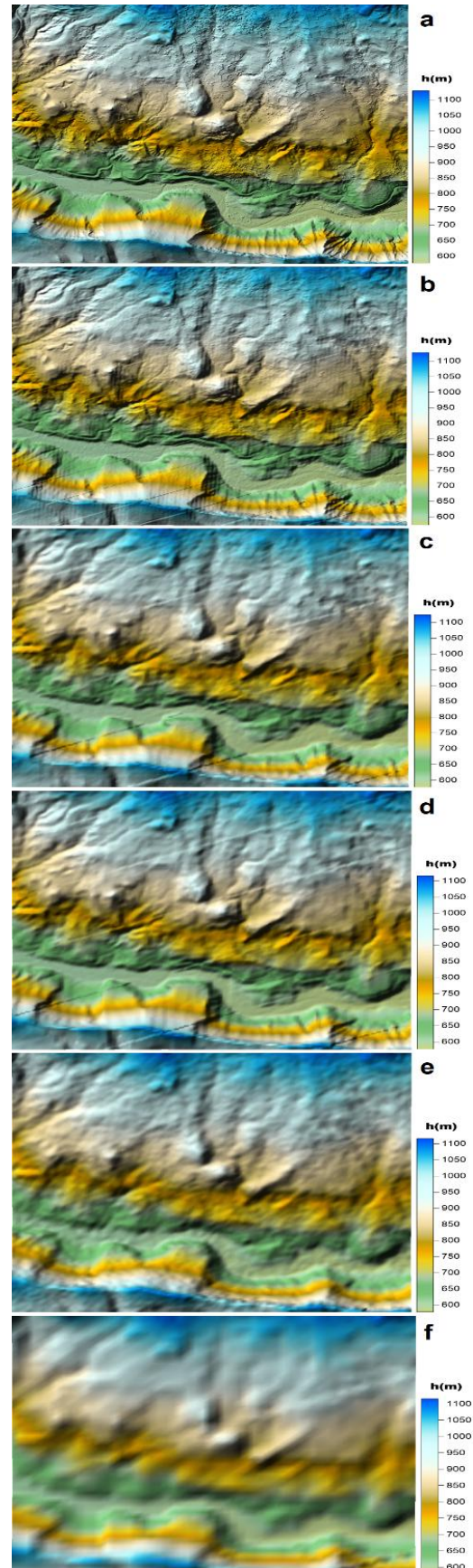


Figure 5. Generated DSMs: (a) REF, (b) TDM12, (c) AW3D30, (d) TDM EDEM, (e) Sentinel-1, (f) TDM90.

Table 3 presents the absolute vertical accuracies of evaluated DSMs, calculated by model-based comparison with the reference DSM. SZ and NMAD results were achieved after elimination of calculated bias values. The $<6^\circ$ represents the uninclined areas and was calculated by $\arctan^{-1}0.1$. Excluded points determines the percentage of pixels which have >50 m height difference from corresponding reference DSM. The results showed that in the entire area the vertical absolute accuracy of TDM12 reaches up to 1 m as NMAD. In addition, TDM EDEM reaches up to 1 m as NMAD in uninclined areas. The excluded points' percentage is minimum in TDM EDEM. As expected, the performance of TDM90 is not as high as the other DSMs due to lower description potential depending on point spacing. In three 30 m global DSMs, TDM EDEM have the highest performance. The general accuracy sequence is $TDM12 > TDM EDEM > AW3D30 > Sentinel-1 > TDM90$. In uninclined areas, the accuracies of all evaluated DSMs are 2 times higher than in entire area. Like in horizontal shifting results, the direction of the bias in Sentinel-1 is inverse in comparison with other DSMs. Figure 6 shows the absolute vertical accuracies of the DSMs, calculated by comparing with the photogrammetric reference DSM as clustered columns for better interpretation.

Evaluated DSM	Bias (m)	SZ without bias(m)		NMAD without bias (m)		Exc. points (%)
		All	SZ $<6^\circ$	All	NMAD $<6^\circ$	
TDM12	1.07	2.13	0.77	1.01	0.60	0.07
AW3D30	0.76	3.68	1.56	2.18	1.31	0.23
TDM EDEM	1.25	3.09	1.35	1.97	1.05	0.01
Sentinel-1	-1.99	4.03	2.63	2.75	2.27	0.12
TDM90	0.15	7.91	3.87	5.04	2.82	0.17

Table 3. Absolute vertical accuracies of evaluated DSMs.

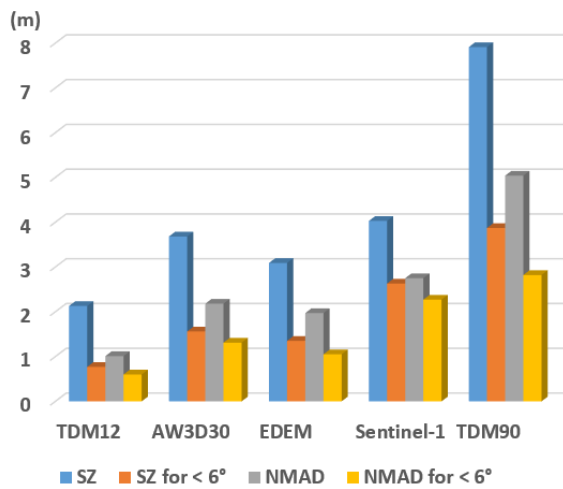


Figure 6. Absolute vertical accuracies of the DSMs, in relation to the photogrammetric reference DSM.

In Figure 7, distribution of height differences between evaluated DSMs and the reference DSM are given as frequency distribution of ΔZ (FDZ) and normal distribution based on SZ, and NMAD. In the first view, abnormal structure of TDM90 FDZ stands out due to several height difference outside the range of ± 8 m distribution interval. Along with TDM12, TDM EDEM draws attention with its FDZ performance despite its 30 m point spacing. Especially in the areas with slope $<6^\circ$, the FDZ, SZ and NMAD distribution performance of the TDM EDEM is very

close to TDM12. The performance of AW3D30 is also remarkable both in entire and uninclined areas. The performance of Sentinel-1 FDZ appears to be somewhat noisy compared to other DSMs except TDM90.

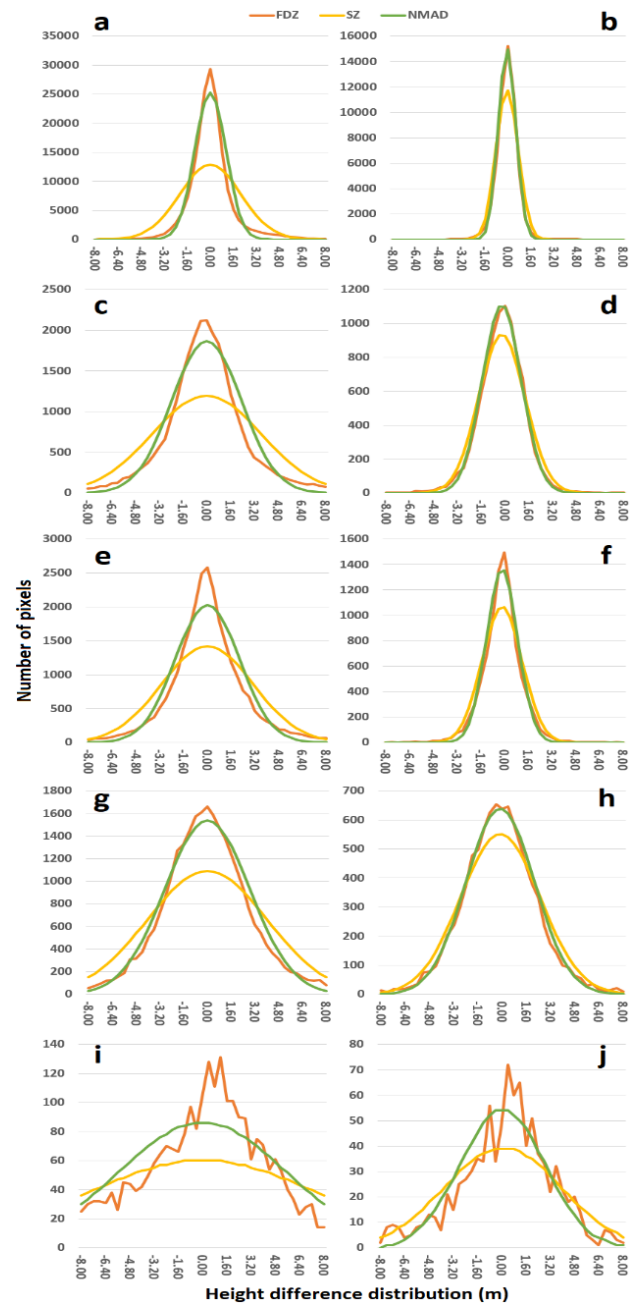


Figure 7. Height difference distribution between evaluated DSMs and the reference DSM: (a) TDM12, (b) TDM12 for slope $<6^\circ$, (c) AW3D30, (d) AW3D30 for slope $<6^\circ$, (e) TDM EDEM, (f) TDM EDEM for slope $<6^\circ$, (g) Sentinel-1, (h) Sentinel-1 for slope $<6^\circ$, (i) TDM90, (j) TDM90 for slope $<6^\circ$.

Figure 8 depicts the pixel-based visual distribution of height differences against the reference DSM. The HEMs were produced in three different scales as ± 50 m, ± 10 m and ± 2 m for better interpretation. The HEMs once again demonstrate the high quality of the TDM12 global DSM. The TDM12 is in ± 2 m coherence with the photogrammetric reference DSM in many regions. Only it has a performance loss in very steep southern part of the study area due to layover, foreshortening and shadow effects. For the other global DSMs, ± 2 m coherence looks very

hard to achieve. However, in ± 10 m scale, HEMs of the DSMs are reasonable. A situation that is different from other results here is that Sentinel-1 DSM has more points in HEMs than other DSMs with 30 m point spacing. This can be interpreted as Sentinel-1 DSM pixels have a certain absolute error but their internal compatibility (i.e., relative accuracy) is higher.

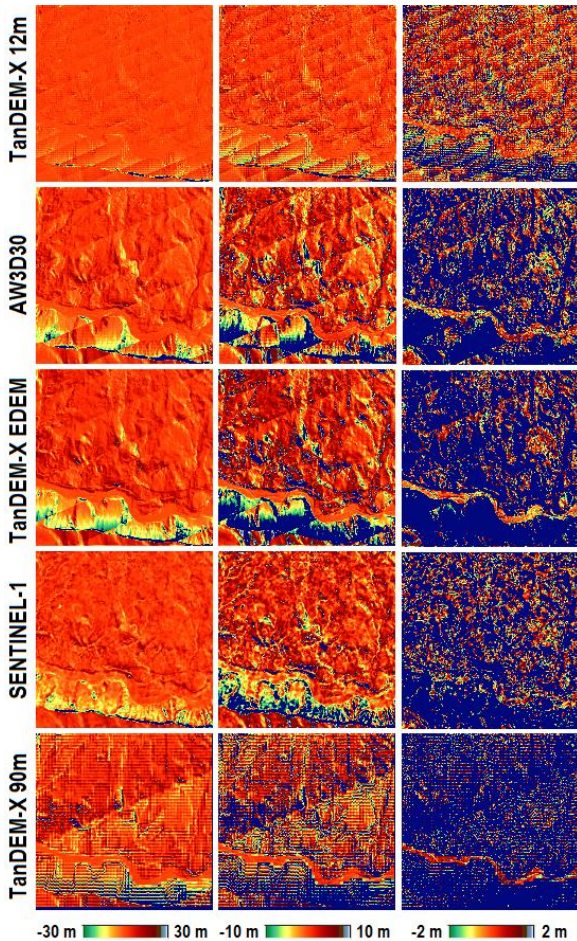


Figure 8. HEMs between evaluated DSMs and the reference DSM (left to right ± 30 m, ± 10 m, and ± 2 m scales).

Figure 9 shows the relative vertical standard deviation of evaluated DSMs. As parallel with HEM interpretation, the RSZ of Sentinel-1 continues steady after 3rd neighbouring pixel to 10th. That means, after a constant value, the interior integrity of the neighbouring pixels is high. Overall, the RSZs of global DSMs are in the same order as the absolute vertical accuracy results, which are TDM12 > TDM EDEM > AW3D30 > Sentinel-1 > TDM90.

Figure 10 illustrates the contour lines produced from the reference DSM and the evaluated DSMs. The contour lines of TDM12 global DSM are almost in the same level of detail as the reference. In addition, the level of detail of AW3D30 global DSM is very close to TDM12 and the reference DSM. The main reason for this case might be the 2.5 m resolution ALOS images that was used for AW3D30 DSM generation. Because, level of detail in the contour lines directly depends on the resolution of the images used for DSM generation. In addition, the DSM based on optical images has only a lower accuracy in steep areas, but no problems with layover.

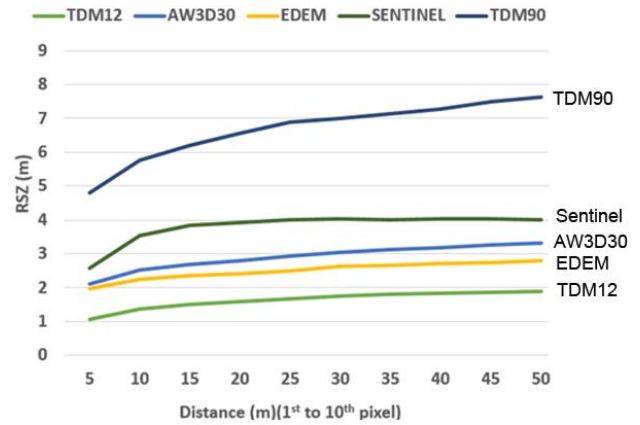


Figure 9. Relative vertical accuracies of evaluated DSMs.

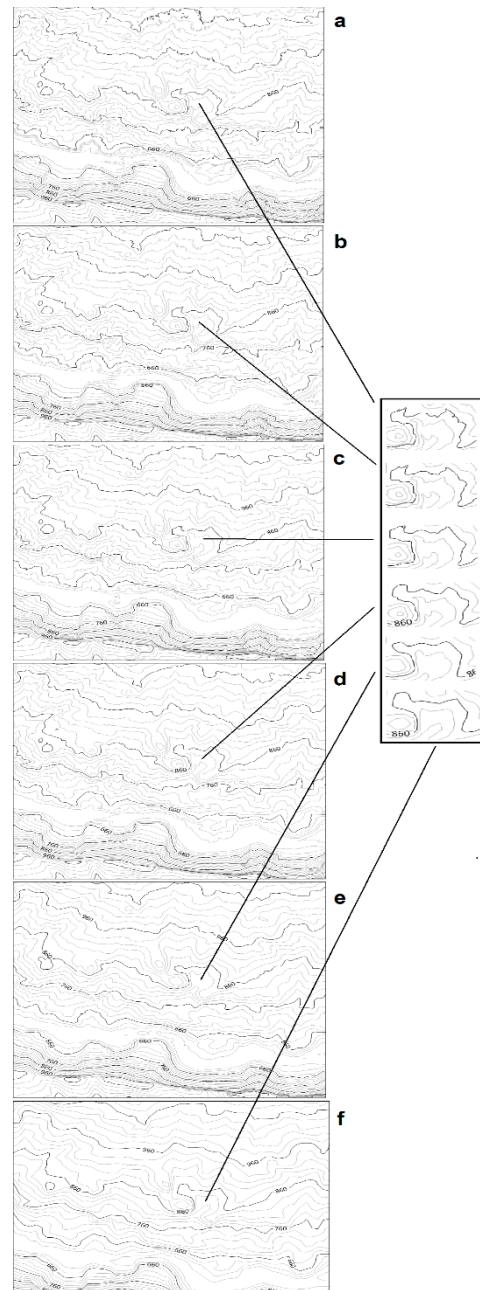


Figure 10. Generated contour lines: (a) REF, (b) TDM12, (c) AW3D30, (d) TDM EDEM, (e) Sentinel-1, (f) TDM90.

Overall, the results of the study demonstrated that TDM12 has higher accuracies against other global DSMs thanks to the smallest point spacing. The absolute and relative vertical accuracies of the TDM EDEM rank second due to the point spacing of 30 m. However, the contour line performance of AW3D30 is better than TDM EDEM with the advantage of 2.5 m prism images used for its generation. Sentinel-1 has the most consistent HEM with the reference among the 30 m models, although it has a constant error that negatively affects statistical accuracy values. Due to 90 m point spacing, the quality of TDM90 is not as high as other global DSMs.

5. Conclusions

In this study, the quality of highly demanded TDM12 and the free of charge AW3D30, TDM EDEM, Sentinel-1 and TDM90 global DSMs were investigated by using 5 m spacing photogrammetric reference model-based by statistical and visual approaches. The quality of a DSM can be assessed considering two main parameters as the accuracy and the morphologic description potential. Accordingly, firstly absolute and vertical accuracy analyses were completed and the morphological performance checked.

The results clearly show the importance of the sensing principle and image properties, imaging geometry, DSMs point spacing and source image resolution. A very important finding was that the TDM12 global DSM showed very high coherence with the 5 m spacing photogrammetric reference model in terms of both accuracy and morphology. On the other hand, the accuracy level of the free TDM EDEM is the second highest after TDM12. However, thanks to the 2.5 m resolution of the ALOS images, AW3D30 has better morphologic representation capability than TDM EDEM. In general, AW3D30 has some advantages in very steep areas, but the accuracy in the areas with lower slope is not as good. The performance of Sentinel-1 is not bad and the RSZ of its height points is strong except for a certain height difference between the reference, nevertheless the absolute accuracy is not as good. According to the accuracy results, the TDM EDEM and AW3D30 DSMs are close to each other. The generated Sentinel-1 DSM just is based on one SAR-image combination, which cannot compete with TDM EDEM, which is based on several SAR image combinations and Sentinel-1 is influenced by the atmospheric changes of taking both used images. TDM90 cannot be recommended due to its lower point spacing, leading to lower accuracy in this rough test area.

Acknowledgements

We would like to thank German Aerospace Center (DLR), European Space Agency (ESA), and Japan Aerospace Exploration Agency (JAXA) for free-of-charge TanDEM-X, AW3D30, and Sentinel-1 data. In addition, thanks are going to Republic of Türkiye, Ministry of National Defence, Directorate General for Mapping to provide reference photogrammetric data and TanDEM-X 12 m data.

References

Baltsavias, E. P., 1999. A comparison between photogrammetry and laser scanning. *ISPRS Journal of photogrammetry and Remote Sensing*, 54(2-3), 83-94.

Chen, X., Sun, Q., Hu, J., 2018. Generation of complete SAR geometric distortion maps based on DEM and neighbor gradient algorithm. *Applied Sciences*, 8(11), 2206.

Hidayatulloh, A., Chaabani, A., Zhang, L., Elhag, M., 2022. DEM study on hydrological response in Makkah City, Saudi Arabia. *Sustainability*, 14(20), p.13369.

Hounam, D., Werner, M., 1999. The shuttle radar topography mission (SRTM). In *Proceedings of ISPRS workshop - Sensors and Mapping from Space*.

Jacobsen, K., 2012. Characteristics of nearly world-wide available digital height models. In *10th Seminar on Remote Sensing and GIS Applications in Forest Engineering*, Curitiba, Brazil, 15-18.

Jacobsen, K., Passini, R., 2010. Analysis of ASTER GDEM elevation models. *The International Archives of the Photogrammetry, Remote Sensing and Spatial Information Sciences*, XXXVIII-Part 1, 38(Part 1).

Kocaman-Aksakal, S., Gruen, A., 2008. Geometric modeling and validation of ALOS/PRISM imagery and products. *International Archives of the Photogrammetry, Remote Sensing and Spatial Information Sciences*, 37(B1), 731-738.

Krieger, G., Moreira, A., Fiedler, H., Hajnsek, I., Werner, M., Younis, M., Zink, M., 2007. TanDEM-X: A satellite formation for high-resolution SAR interferometry. *IEEE Transactions on Geoscience and Remote Sensing*, 45(11), 3317-3341.

Nikolakopoulos, K., Kyriou, A., 2015. Preliminary results of using Sentinel-1 SAR data for DSM generation. *European Journal of Geography*, 6(3), 52-68.

Rossi, C., Gernhardt, S., 2013. Urban DEM generation, analysis and enhancements using TanDEM-X. *ISPRS Journal of Photogrammetry and Remote Sensing*, 85, 120-131.

Sefercik, U.G., Jacobsen, K., 2006. Analysis of SRTM height models. In *Fifth International Symposium Turkish-German Geodetic Days*, Technical University, Berlin, Germany, 28-31.

Sefercik, U. G., Glennie, C., Singhania, A., Hauser, D., 2015. Area-based quality control of airborne laser scanning 3D models for different land classes using terrestrial laser scanning: sample survey in Houston, USA. *International Journal of Remote Sensing*, 36(23), 5916-5934.

Sefercik, U.G., Yastikli, N., 2016. ALS model-based comparison of Cosmo-SkyMed and TerraSAR-X HS DSMs on varied land forms. *Journal of Spatial Science*, 61(1), 119-131.

Sefercik, U.G., Buyuksalih, G., Atalay, C., Jacobsen, K., 2018. Validation of Sentinel-1A and AW3D30 DSMs for the metropolitan area of Istanbul, Turkey. *PFG-Journal of Photogrammetry, Remote Sensing and Geoinformation Science*, 86, 141-155.

Sefercik, U.G., Buyuksalih, G., Atalay, C., 2020. DSM generation with bistatic TanDEM-X InSAR pairs and quality validation in inclined topographies and various land cover classes. *Arabian Journal of Geosciences*, 13, 1-15.

Stamatiou, C.C., Liampas, S.A.G., Drosos, V.C., 2018. Vertical accuracy comparison of ALOS AW3D30 DSM and trigonometric survey points. In *Sixth International Conference on Remote Sensing and Geoinformation of the Environment (RSCy2018)*, 10773, 532-537.

Yastikli, N., Sefercik, U. G., Esirtgen, F., 2014. Quantitative assessment of remotely sensed global surface models using various land classes produced from Landsat data in Istanbul. *Chinese Geographical Science*, 24, 307-316.

Wessel, B., 2016. TanDEM-X Ground Segment– DEM Products Specification Document. EOC, DLR, Oberpfaffenhofen, Germany, Public Document TD-GS PS-0021, Issue 3.1, 2016. [Online]. Available: <https://tandemx-science.dlr.de/>.

Wessel, B., Huber, M., Wohlfart, C., Marschalk, U., Kosmann, D., Roth, A., 2018. Accuracy assessment of the global TanDEM-X Digital Elevation Model with GPS data. *ISPRS Journal of Photogrammetry and Remote Sensing*, 139, 171-182.